Paraboloidal Dish Arrays with Steam Energy Transport Network

Jeff Cumpston[1], Keith Lovegrove[2], José Zapata[3], and John Pye[4]

[1] B science (hons), B Photonics, PhD Student. Address: Department of Engineering, Australian National University, Canberra, ACT, 0200, Australia, +61 2 6125 3072, jeff.cumpston@anu.edu.au

[2] PhD, Consultant, IT Power Australia, Address: PO Box 6127, O'Connor, ACT, 2602, Australia

[3] B Engineering (hons), PhD Student. Address: Department of Engineering, Australian National University, Canberra, ACT, 0200.

[4] PhD, Lecturer, Address: Department of Engineering, Australian National University, Canberra, ACT, 0200.

Abstract

A model for calculating annual system costs that are associated with collector placement for an array of paraboloidal dishes with a steam energy transport network is presented. All possible lattices that define a regularly-spaced dish-array within a discrete finite parameter space are applied to a previously proposed array shape and energy transport network topology. An optimum lattice, subject to constraints introduced by shading and losses associated with the energy transport network, is presented. A brief analysis of the lattice suggests that summer- and winter-solstice sunrise azimuth angles may inform the placement of such arrays.

1. Introduction

Dish concentrators are theoretically capable of higher concentration ratios than other solar-thermal collector technologies. With a high concentration ratio, collection losses such as radiation and convection losses from cavity receivers can be minimised. Dish concentrators do not suffer from cosine losses (with respect to concentrator aperture area), blocking losses, and atmospheric attenuation of reflected solar radiation is negligible. There are, however, energy losses and pipework costs associated with the spatially distributed collector system layout.

The ANU Solar Thermal Group has constructed a 500m^2 paraboloidal collector that is currently used for power generation using a DSG energy transport system [1]. Commercialisation plans are to fabricate arrays of these dishes and have them connected via a steam pipe network to a single central power block.

Array shapes have been proposed by Carden and Bansal [2] based on optimisations of energy transport networks (see [3]) for steam delivery to regularly-spaced point-focus distributed receivers (PFDR). Array costs were minimised with respect to optimal pipe dimensions and pipe insulation thickness, determined subject to fluid friction and thermal energy losses from the steam medium. Carden and Bansal cited dish spacing to render shading loss as negligible, citing the work of Osborn (1980)[1] for a fixed rectangular spacing. However, by quantifying and determining an admissible shading loss for a reduction in pipe length, an improvement in annual array performance can be seen by altering dish-separation [5].

Previous studies on shading have applied constraints when defining the lattice by which the collectors are arranged. Pons and Dugan [6] quantify and minimise annual shading fraction in a field of dish-Stirling collectors for a range of ground-cover ratios in arrays arranged subject to a rectangular lattice constraint. These results were reproduced by Meller [7], with improvements made to the computation algorithm. Igo [8] performs an economic analysis of a large dish-Stirling field by simulating a dish-field with a fixed ground-cover ratio constraint. Annual shading fraction for dish-lattices with staggered rows is simulated and it is found that an unstaggered (rectangular) layout corresponds to minimal shading. Edwards [9] presents a study that models the shading and pipe network losses for a dish field with collector arrangement constrained to square lattices of changing dimension. Also included was a study of lattice rotation for a given lattice side-

1 This reference cannot be retrieved. Please see appendix in thesis by Fraser [4]

length, and it was found that rotated lattices may increase annual energy collection of a dish-field by about 1%. This may indicate that rectangular or square lattices do not represent the optimal basis for the arrangement of an array of PFDR's.

In this study, the energy transport network proposed by Carden and Bansal [2] is used as the basis for determining the pipe losses in an array of PFDR's. A technique for evaluating the system costs associated with this pipe network and the shading from adjacent collectors is presented. The losses are evaluated for an unconstrained set of possible dish-lattice arrangements after an introduction to how this set is defined is presented. An example lattice for which the minimum associated system costs were found is presented.

2. Proposed Dish Array

The energy transport network follows a tree-like structure that was proposed by Carden and Bansal [2], shown in Figure 1. The major axis (denoted in this paper with subscript *maj*) is that associated with a higher system cost which in this case, with 418 links, corresponds to the vertical axis seen in Figure 1. The minor axis (denoted in this paper with subscript *min*) is the axis that runs perpendicular to the major axis and has the least system cost, with 92 links, associated with it. These definitions are used to align with lattice basis vectors defined in Section 3.

The pipe sizing for each link in the network is determined by the nominal mass flow carried to the central block at each point. Lines closer to the edge of the field are thus smaller, as they are carrying the load from a smaller number of dishes, whereas lines closer to the center of the field are larger and require more insulation and larger pipes in order to convey superheated steam from a greater number of dishes. Based on this, insulation thickness and pipe size are optimised for the required mass flow in each link subject to the model presented in Section 4.2.

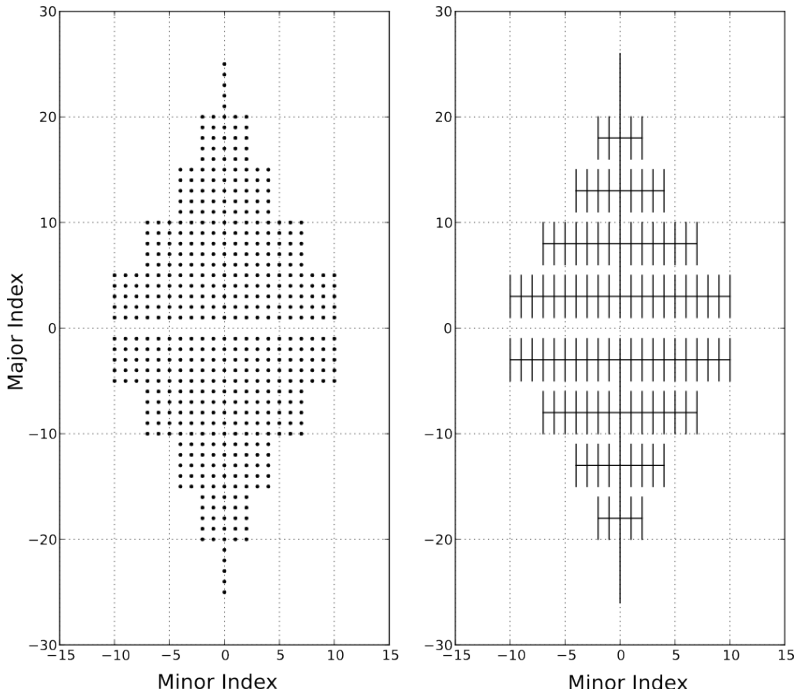

Figure 1. Dish-field array. Each dot represents a paraboloidal dish (left) and lines represent the underlying energy transport network (right). Pipe links enter the power block at (0,1) and (0,-1) for the top and bottom half, respectively.

3. Dish Position Parameter Space

Inter-dish proximity will determine the length, and therefore, the system costs associated with the pipe network in the dish-array. Dish lattice arrangements will also determine the amount of shading that each collector experiences due to adjacent collectors. This section describes the parameter space for defining the simulated lattices used in this study.

In order to evaluate the influence of shading and the energy transport network on system costs, a large range of possible dish array spacing combinations was generated . A lattice is formed for each array combination by placing two dishes at arbitrary distances from a reference dish (Figure 2).

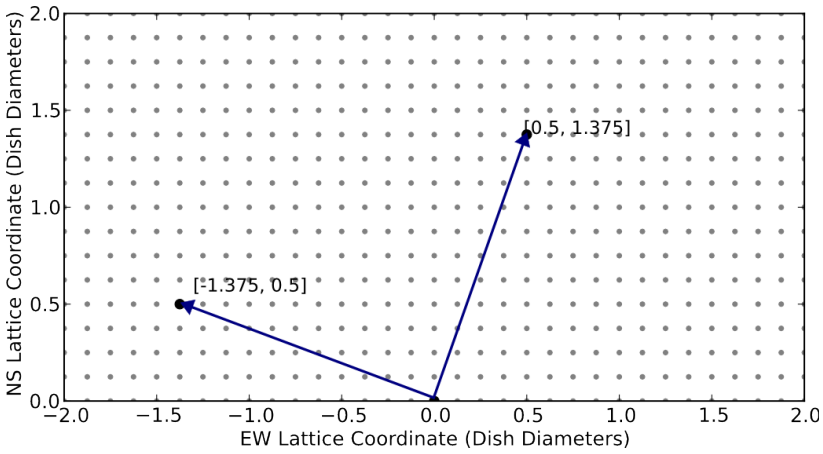

Figure 2. Parameter space for defining lattice vectors. Each site (grey dot) is a candidate for defining lattice basis vectors. The vectors pictured show an example basis.

A set of all possible unique combinations of vectors for the parameter space exhibited in figure 2 is defined. This represents a relaxation of all spacing constraints for regularly-spaced dish-arrays, within this discrete parameter space, such as those cited in Section 1.

The defined set of vector combinations may represent duplicate lattice bases, however, as the uniqueness of basis vectors does not always imply a uniquely defined lattice. A check for duplicates is conducted by taking the following matrix transformation between two lattice bases in the list:

$$\begin{pmatrix} \vec{v}_{min} \\ \vec{v}_{maj} \end{pmatrix} \begin{pmatrix} A & B \\ C & D \end{pmatrix} = \begin{pmatrix} \vec{p} \\ \vec{q} \end{pmatrix} \quad (1)$$

where $\vec{v}_{maj}$ and $\vec{v}_{min}$ comprise a chosen lattice basis and $\vec{p}$ and $\vec{q}$ some other basis to be assessed. A, B, C, and D can be determined from the vector entries. $\vec{p}$ and $\vec{q}$ represent a duplicate basis of $\vec{v}_{maj}$ and $\vec{v}_{min}$ when A, B, C, D are integers and,

$$\begin{vmatrix} A & B \\ C & D \end{vmatrix} = 1 \quad (2)$$

One of the bases in the defined set is chosen for $\vec{v}_{maj}$ and $\vec{v}_{min}$ and each remaining lattice basis in the defined set is substituted in for $\vec{p}$ and $\vec{q}$ to determine if it is a duplicate. Once the duplicates of $\vec{v}_{maj}$ and $\vec{v}_{min}$ are removed, the next remaining lattice basis in the set is considered as the candidate for a duplicate search, and so on until all duplicates are removed.

The remaining lattice basis vectors are then reduced to the shortest possible pair of basis vectors that define

the lattice by applying the LLL basis reduction [10] test over all the possible integer linear combinations of the current lattice basis vectors until the basis is found. Reduced lattice bases have vector magnitudes that represent the shortest path between adjacent dishes for a given lattice. As such, reduced lattice basis vectors can be used to define pipe links between dishes.

$\vec{v}_{maj}$ is defined as the vector along which the major axis of the array is directed, and is aligned with the shortest vector of the two lattice basis vectors; $\vec{v}_{min}$ along the other axis. This ensures that the pipes along the axis that represents the most cost is minimised in length and vice-versa.

4. Shading and Pipe Network Constraints

A general formulation of the annual costs, α_t , of the proposed dish field that arise as a function of dish proximity is represented by,

$$\alpha_t(\vec{v}_{maj}, \vec{v}_{min}) = \alpha_s(\vec{v}_{maj}, \vec{v}_{min}) + \alpha_{p,maj}(\vec{v}_{maj}) + \alpha_{p,min}(\vec{v}_{min}) \quad (3)$$

where α_s is total annual solar energy lost as a result of inter-dish shading across all of the dishes in the field, $\alpha_{p,maj}$ is the equivalent cost due to the pipe network over a year of operation in the major axis, and $\alpha_{p,min}$ is the same for the minor axis. Pipe loss coefficients are separated in this way because they are a function of the independent vectors that define the basis of the particular dish-field lattice. These coefficients are expanded as follows,

$$\alpha_s = \sum_{i=1}^{N_s} DNI_i \sum_{j=1}^{N_d} A_{s,ij}(\vec{v}_{maj}, \vec{v}_{min}) \quad (4)$$

$$\alpha_{p,maj} = Q_{p,maj} \|\vec{v}_{maj}\| \quad (5)$$

$$\alpha_{p,min} = Q_{p,min} \|\vec{v}_{min}\| \quad (6)$$

Where N_d is the number of dishes in the dish-field, N_s is the number of time samples used in the simulation. $A_{s,ij}$ is the shaded area on a given dish for the given timestep, and is determined by a shading model that calculates dish-overlap as a function of dish-position and sun-position. Direct Normal Irradiation (*DNI*) may be provided either by weather data or by clear-sky radiation models. The Q_p coefficients represent the total annual 'loss' from the pipes in the major (maj) and minor (min) axes respectively. In this case, 'loss' refers to an equivalent energy loss that corresponds to thermal losses, friction losses, pipe material costs, and pipe insulation costs. This is discussed further in Section 4.2.

4.1 Shading Costs

The collectors directly adjacent to the collector of interest are known as first-order neighbours. For a regular 2-Dimensional lattice there are a maximum of 8 first-order neighbours (see Figure 4 for an example of a first-order neighbourhood), though dishes with absent neighbours that are close to the edge of the array are represented by different neighbourhood combinations.

The shading algorithm is described by Meller [7]. α_s was calculated by finding $A_{s,ij}$ for each dish for each timestep. The solar vector is used as the vantage point for the calculation. The sun position may be determined by an analytical algorithm. The Grena [11] algorithm is currently implemented in this model. From this vantage, the area of the dishes in front of the dish of interest that obscure it represent shading. Figure 3 shows an example first-order neighbour shading calculation for a given timestep as viewed from the sun.

The calculated shading area reduces the power collected by the dish for the given time step. The shaded area

is multiplied by the DNI and integrated over each timestep in order to calculate the total energy lost for the annual simulation. The energy is expressed in the same units as that calculated for pipe loss so that it may be used in Equation 3.

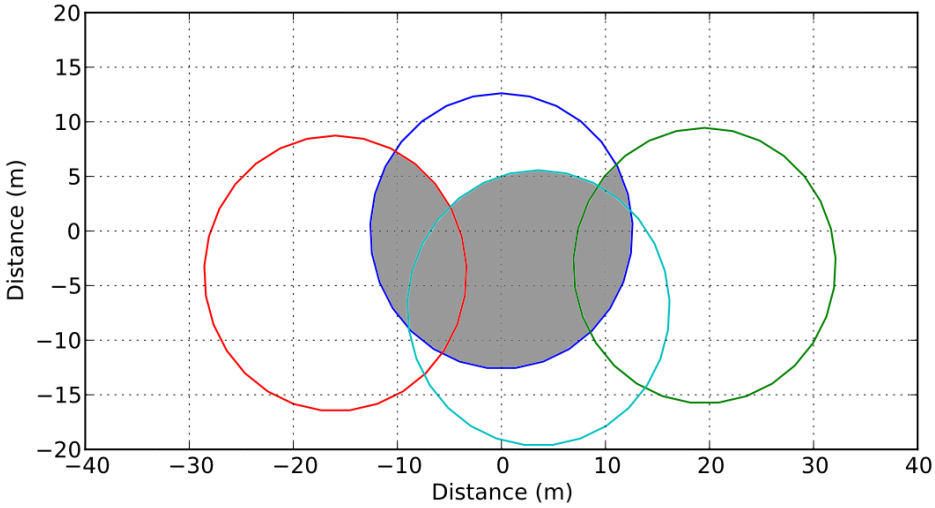

Figure 3. Graphical representation of polygon overlap in the sun-view coordinate system for a discrete time sample. Overall shading is the area of the union of shade polygons that are determined by calculating the intersection of each polygon with the central polygon.

4.2 Energy Transport Network Costs

In the simulated pipe network, the dishes are linked in parallel, such that each link in the feedwater line must carry the mass flow required for all downstream dishes, and each link in the steam line carry the flow back from these dishes. This model closely follows that presented by Lovegrove [12].

The length dependent costs associated with the energy transport network were simulated. The annual integrated costs, Q_p , associated with each basis vector of the energy transport network are determined by,

$$Q_p = \sum_{n=1}^{N_l} \dot{Q}_{in,n} t + \dot{Q}_{th,n} t + \dot{Q}_{st,n} t + \sum_{i=1}^{N_s} \dot{Q}_{pd,n}(DNI_i) \qquad (7)$$

where N_l is the number of pipe links aligned with the respective basis vector, and N_s represents the number of timesteps.

All costs and losses are expressed as an equivalent heat loss per unit length, in order for them to be compared quantitatively. $\dot{Q}_{in}$ represents the price of investment in insulation, converted into an equivalent thermal loss subject to electricity prices and annual interest on investment. Similarly, $\dot{Q}_{st}$ is the same for the price of pipe steel. $\dot{Q}_{th}$ is heat transfer from the fluid medium to the environment, and $\dot{Q}_{pd}$ is the pressure drop along the length of the pipe. All of these have units of power per unit length.

The variable *t* is the annual operational time of the power plant as determined by average total annual sunlight hours for the simulated site [13]. $\dot{Q}_{pd}$ is a function of *DNI* and is time-dependent, as the model simulates changes in mass flow to maintain a constant steam outlet temperature from each dish for a given *DNI*.

For a given lattice basis, Q_p is evaluated for each basis vector and represents the equivalent annual energy loss per unit basis-vector-length. All pipe links that lie in the direction of a given basis vector are included in this coefficient.

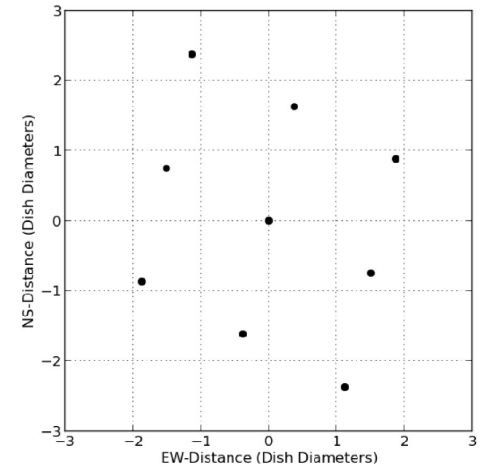

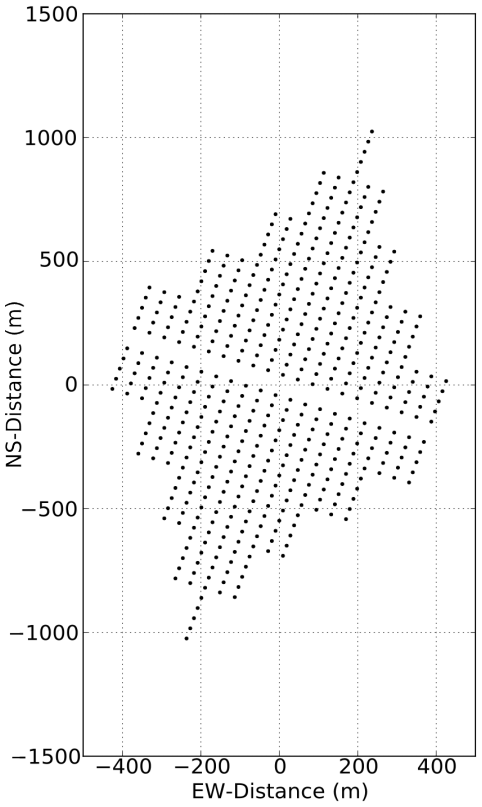

Figure 4. The calculated optimum first-order lattice for the simulated energy transport network and power plant site (top) and the arrangement of the dishes comprising the power plant (bottom).

Implicit in these loss factors are pipe dimensions for each pipe link that have been determined through optimising for reduced cost over all of these mechanisms, subject to many input parameters. The pipe dimensions are determined to minimise equivalent energy loss for 'ideal' insolation conditions of $1\mathrm{kW/m^2}$ during operational hours.

5. Example Solution

A simulation was performed using the pipe network parameters specified by Lovegrove [13]. This is done for all of the lattice combinations generated, as defined in Section 3, in order to find the lattice that corresponds to the lowest annual length-dependent equivalent energy loss for the defined dish array and energy transport network.

The dish-aperture shape for the simulation was circular (Figure 3). Hourly Meteonorm data taken from TRNSYS for Canberra, Australia was used for the DNI data. The resulting lattice is shown in Figure 4, along with the new array configuration defined by the lattice, with distances in metres.

The basis vectors for this lattice are:

$$\vec{v}_{min} = (0.375, 1.625)$$

$$\vec{v}_{maj} = (-1.5, 0.75)$$

in units of dish-diameters.

The ground-cover ratio for this lattice is 0.287.

The distances between the dishes are determined by the energy transport network constraint, and 3.27% of available annual solar energy for the year is admitted to shading in order to reduce pipe network losses by reducing pipe length.

Pipe network losses were calculated at 15.7% of available annual solar energy. This number is included for completeness, though its calculation was performed using data taken directly from Lovegrove [12], and should be updated if a more accurate quantitative study is required.

5.1 Analysis of Lattice Shape

The reason for the skewing of the lattices in this fashion may be related to the seasonal variation in the sun path. As a first investigation into this, the azimuth angles of the ESE and ENE dishes in figure 4 (top) were calculated. The ESE dish is situated approximately 26.5 degrees South of East and the ENE dish is situated at approximately 25.0 degrees North of East.

Due to its sinusoidal (to first order) seasonal variation, the sun path for a given day varies the least during the summer and winter months. The summer and winter solstice days were therefore considered to represent the approximate sun path throughout these respective seasons.

The azimuth angle of the sun at sunrise at the summer solstice (21st December, 2012), calculated using the Grena sun-position algorithm, is approximately 29.6 degrees South of East. For this same day, the solar altitude angle is 3.6 degrees at the azimuth angle of the ESE dish, a time of almost negligible DNI. By the time the azimuth angle of the sun corresponds to that of the ENE dish, its altitude angle is 67.0 degrees; no shading is possible due to the high solar elevation.

The azimuth angle of the sun at sunrise at the winter solstice (21st June, 2013) is approximately 28.7 degrees North of East and its path does not cross the azimuth angle of either of the easterly dishes in question.

Shading from the westerly dishes will exhibit the same behaviour observed in the easterly dishes discussed above.

The dish most directly north is slightly tilted away from north. This will reduce shading during times of peak DNI.

Due to its distance from the centre, the northernmost dish is not likely to shade the center dish at any time. The remaining two southern-most dishes will not contribute any shading as the sun is below the horizon for these azimuth angles.

The angles at which the ESE and ENE dishes are placed are very close to the sunrise angles for summer and winter, respectively. The analysis above suggests that this may be used as a guideline for placing dishes into regular arrays.

6. Model Assumptions

Annual Calculations are performed at hourly time-intervals. This may introduce a systematic error into the annual shading integration when the geometry of the dish face is comparable or smaller than the movement of the projected shade area between time intervals.

Dish positions are constrained to a regular lattice. It is expected that further investigation into this problem will prove that dishes linked by pipes of a smaller diameter (ie. those at then end of branches) that introduce less energy transport cost per length may require larger spacing.

Possible Lattice positions are determined by the discrete parameter space. The resolution of the parameter space simulated was 0.125 dish diameters to limit computation times. Simulations at higher resolutions can be conducted around the vicinity of the calculated minimum, to refine results.

Investigations of lattice alterations in the absence of weather effects may also be conducted using a clear-sky radiation model such as the Hottel, Meinel, or Allen models [14].

Losses from pipe links are constant along length of given link. Of the four loss mechanisms quantified, friction and thermal losses have a marginal cost that changes with respect to pipe length. The model could be extended to incorporate a model of pipe links that accounts for changes in frictional- and heat-transfer-costs per unit length as a function of pipe length.

Pipe-link dimensions and associated losses are determined for the nominal mass flow rate required for 'ideal' insolation conditions of $1\mathrm{kW/m^2}$ over the total annual sunlight hours, however optimisation of pipe dimensions to reduce costs based on frictional mean flow, rather than this reference flow, would reduce costs.

First-order neighbour calculations are used for shading. The validity of this approach has been verified by Meller [7] for rectangular lattices, but asymmetries in first-order lattices shapes are observed when they are skewed in the way that is allowed by the lattice basis definitions in this study. A dynamic neighbourhood definition that calculates shading from all possible dishes could be implemented to ensure maximum accuracy, at the expense of more computation time.

7. Conclusions

Dish-lattice constraints seen in previous studies were relaxed within a defined parameter space in order to investigate new possibilities in field arrangements of two-axis tracking collectors. Subject to the assumptions of the shading and energy transport model, an optimised dish lattice was determined for reduction of length-dependent system losses. This was performed for a previously proposed dish-array and associated pipe network.

As a result of this simulation, insight was gained into the placement of two-axis tracking collectors for reduction of position-dependent losses. The approximate respective azimuth angles of the summer and winter sunrise may help to define their placement.

Parameters used in this model, particularly those with which the pipe network was simulated, can be updated from those in this study in order to perform a more accurate quantitative study of these loss mechanisms and dish placement. This should enable comparison with existing solar-thermal technologies and this is a goal for the future.

Other future work will determine the extent to which allowing for all possible lattice configurations has reduced the total system loss.

The simulation program can easily accommodate any dish silhouette, site location, array shape, steam transport network and heat-transfer fluid.

Acknowledgements

I would like to thank my co-authors for their help with this study. Thanks to Dr. Keith Lovegrove for his insight and providing me with a model to extend my shading program. Thanks to Jose Zapata for his constant enthusiasm, unwavering good nature and for taking time to understand my problem enough to make valuable suggestions. Thanks to Dr. John Pye for sharing his wealth of knowledge, open door, and long-discussion sessions about a range of topics.

References

[1] K. Lovegrove, G Burgess, J. Pye, A new 500 m^2 paraboloidal dish solar concentrator, Solar Energy, 85, (2011), 620 - 626.

[2] P. Carden, P. Bansal, Optimisation of steam-based energy transport in distributed solar systems, Solar Energy, 49, (1992), 451 – 461.

[3] P. Carden, P. Bansal, Computer Software for Optimum Energy Transport Layouts for Distributed Solar Systems, Proceedings of Australia and New Zealand Solar Energy Society Annual Conference, 1, (1987), 143-151.

[4] P. R. Fraser, Stirling Dish System Performance Prediction Model, PhD Thesis, University of Wisconsin-Madison, (2008).

[5] J Cumpston., J Pye., Shading Calculations for the Big Dish, Proceedings of SolarPACES 2011, Granada, Spain, Sept. 20-23 (2011)

[6] R. L. Pons, A. F. Dugan, The Effect of Concentrator Field Layout on the Performance of Point-Focus Distributed Receiver Systems, Journal of Solar Energy Engineering, ASME, 106, (1984), 35-38.

[7] Y. Meller, Analytically calculating shading in regular arrays of sun-pointing collectors, Solar Energy, 84 (2010), 1967 – 1974.

[8] J. Igo, C. E. Andraka, Solar Dish Field System Model for Spacing Optimization, Proceedings of Energy Sustainability 2007, (2007).

[9] B. P. Edwards, Shading and spacing in paraboloidal collector arrays, Solar Energy, 21, (1978), 435 – 439.

[10] Lenstra, A. K., Lenstra, H. W., Jr., Lovász, L. Mathematische Annalen, 261 (1982) 4: 515–534.

[11] Grena, R. An algorithm for the computation of the solar position, Solar Energy, 82, (2008), 462 - 470

[12] K. Lovegrove, Heat Transport Network for the Tennant Creek Solar Thermal Power Station, Unpublished, (1993), Appendix.[2]

[13] Australian Bureau of Meterology, Climate of Canberra Area, viewed 17 August 2012, <http://www.bom.gov.au/nsw/canberra/climate.shtml>.

[14] B. L. Kistler, A User's Manual for DELSOL3, Sandia National Laboratories (1986), viewed 17 August 2012, <http://prod.sandia.gov/techlib/access-control.cgi/1986/868018.pdf>

2 Please inquire with the primary author of the current paper about this publication.